Covalently linked adenovirus-AAV complexes as a novel platform technology for gene therapy

Logan Thrasher Collins,[1,2] Wandy Beatty,[3] Paul Boucher,[2] Buhle Moyo,[4] Michele Alves-Bezerra,[5] Ayrea Hurley,[5] William Lagor,[6] Gang Bao,[4] David T. Curiel,[2,*] Zhi Hong Lu[2]

[1]Washington University in St. Louis Department of Biomedical Engineering; [2]Washington University in St. Louis Department of Radiation Oncology; [3]Washington University in St. Louis Department of Molecular Microbiology; [4]Rice University Department of Bioengineering; [5]Baylor College of Medicine Department of Molecular Physiology and Biophysics; [6]Baylor College of Medicine Department of Integrative Physiology, [*]Corresponding Author.

Abstract: Adeno-associated virus (AAV) has found immense success as a delivery system for gene therapy, yet the small 4.7 kb packaging capacity of the AAV sharply limits the scope of its application. In addition, high doses of AAV are frequently required to facilitate therapeutic effects, leading to acute toxicity issues. While dual and triple AAV approaches have been developed to mitigate the packaging capacity problem, these necessitate even higher doses to ensure that co-infection occurs at sufficient frequency. To address these challenges, we herein describe a novel delivery system consisting of adenovirus (Ad) covalently linked to multiple adeno-associated virus (AAV) capsids as a new way of more efficiently co-infecting cells with lower overall amounts of AAVs. We utilize the DogTag-DogCatcher (DgT-DgC) molecular glue system to construct our AdAAVs and we demonstrate that these hybrid virus complexes achieve enhanced co-transduction of cultured cells, including primary cells. This technology may eventually broaden the utility of AAV gene delivery by providing an alternative to dual or triple AAV which can be employed at lower dose while reaching higher co-transduction efficiency.

Introduction

Although adeno-associated virus (AAV) gene therapy has shown enormous promise and led to eight clinically approved treatments,[1–4] it is consistently hampered by the vector's low DNA packaging capacity of 4.7 kb. Great effort has gone into developing dual AAV systems, which deliver two parts of a therapeutic gene in separate capsids that aim to co-infect the same cells.[5–8] Analogous triple AAV systems have also been explored.[9,10] Dual and triple AAV systems can recombine their split genes into complete form through mechanisms of DNA trans-splicing, RNA trans-splicing, or protein splicing via split inteins.[6,8] However, dual and triple AAVs typically require higher doses to achieve efficient co-transduction of cells, especially when systemic administration is necessary.[11] This makes sense since the likelihood of two or three cargos reaching the same cell should roughly correspond to the proportion of a single cargo reaching the cell squared or cubed respectively. Most dual or triple AAV strategies have therefore focused on applications where local administration into target tissues is possible such as retinal gene therapy.[6,8–10] Another drawback of dual and triple AAVs is that they can cause production of partial protein products in cells that did not receive all of the cargos.[6] As these partial proteins are often translated in even larger quantities than the desired therapeutic protein, they can lead to significant toxicity. New approaches for mitigating the problems associated with dual and triple AAV gene therapy would greatly advance the applicability of AAVs for treating conditions that necessitate delivery of large transgenic sequences.

To address these challenges, we herein construct an entirely new type of gene delivery system "AdAAV" which consists of a larger (about 100 nm diameter) Ad capsid decorated by

numerous smaller (about 25 nm diameter) covalently anchored AAV capsids **(Figure 1A)**. In the wild, adenovirus (Ad) and adeno-associated virus (AAV) are "associated" only by virtue of the AAV's dependence on Ad machinery to replicate itself.[12] Their association has not previously involved a physical linkage between the capsids of these types of viruses. By leveraging DogTag-DogCatcher (DgT-DgC) molecular glue peptides,[13] we have constructed the novel biological AdAAV complex. Specifically, AAVs are covalently anchored to the Ad via the isopeptide bond which spontaneously forms between the DgT and DgC peptides in a highly efficient and specific fashion. We engineered Ad5 to bear a DgC fusion on its pIX capsid protein and we engineered AAV-DJ to possess DgT insertions in all of its VP2 proteins and in some of its VP3 and VP1 proteins. AdAAVs facilitate strong co-transduction of cultured cells **(Figure 1B)** even at low multiplicity of infection (MOI). AdAAVs thus represent a new vehicle for enhancing cellular co-transduction in AAV gene therapy.

We envision AdAAV as a way of circumventing the efficiency and dosage limitations of dual or triple AAV gene therapy. By physically linking the AAVs to an Ad core, they improve co-transduction efficiency for multiple cargos into the same cell as compared to when the Ads and AAVs are separated. It should be noted that even without physical linkage, the presence of the Ad improves the transduction efficiency of the AAVs, though to a lesser extent. This is likely due to the helper functions provided by the Ad to the AAV. The overall effect is to drastically lower the dose of viruses needed to achieve efficient co-transduction. Although here we only deliver a single AAV cargo and a single Ad cargo, the high number of AAVs we observed linked to each Ad indicates that the technology should easily extend to co-delivery of both the Ad cargo and more than one AAV cargo. AdAAVs may conceivably even open the door to co-delivery of four or more distinct AAV cargos in addition to any cargos encoded by the Ad's DNA. As a platform technology, AdAAV will have immense versatility. In addition to enhancing dual and triple AAV systems, AdAAV may also eventually facilitate multigenic gene therapy for complex diseases[14–16] and/or enable delivery of multigenic circuits that offer safer and more precise treatments through dynamic responses to changing environmental conditions in real time.[17–19] Our studies here suggest that AdAAVs will provide a powerful new delivery system to the toolkit of gene therapy which has advantages for co-delivery of large split transgenes and for delivery of multiple genetic cargos.

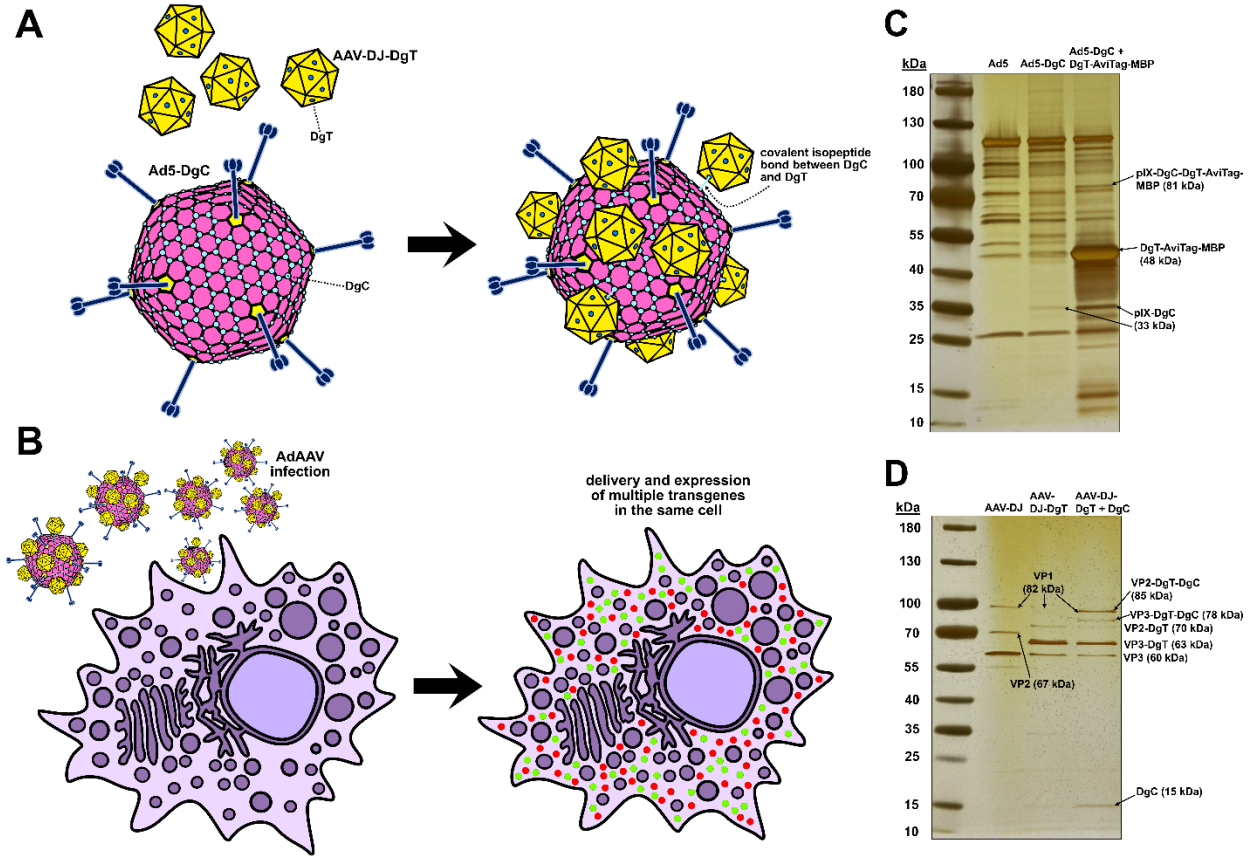

Figure 1 (A) Schematic of AdAAV complex assembly and organization. Ad5-DgC has 240 pIX-DgC proteins in its capsid, while AAV-DJ-DgT incorporates a stochastically varying number[20] of VP2-DgT, VP3-DgT, and VP1-DgT proteins in its capsid. Upon mixing, Ad5-DgC reacts with AAV-DJ-DgT to form covalent isopeptide bonds between their DgC and DgT peptides. **(B)** Schematic of AdAAVs infecting a cell and expressing multiple transgenes as seen in this study. AdAAVs may in the future improve delivery of split transgenes too large to fit within a single AAV capsid. **(C)** Silver stain SDS-PAGE gel of Ad5, Ad5-DgC, and Ad5-DgC mixed with 20-fold excess (relative to pIX-DgC copies) DgT-AviTag-MBP. In the latter lane, the reaction between pIX-DgC and DgT-AviTag-MBP produces a new band at 81 kDa corresponding to pIX-DgC-DgT-AviTag-MBP. **(D)** Silver stain SDS-PAGE gel of AAV-DJ, AAV-DJ-DgT, and AAV-DJ-DgT mixed with 20-fold excess (relative to VP2-DgT copies) DgC. In the latter lane, the reactions of DgC with VP2-DgT and VP3-DgT produce new bands at 78 kDa and 85 kDa. No VP1-DgT or VP1-DgT-DgC is visible, indicating that these proteins were very low in copy number.

Results

As a first step for constructing AdAAVs, we modified capsid proteins in Ad5 and AAV-DJ to incorporate the DgC and DgT peptides respectively. We decided to fuse DgC to the minor Ad capsid protein pIX since alterations to this protein are typically less disruptive to production and infectivity compared with the other capsid proteins.[21] With 240 copies of pIX per Ad capsid, the Ad5-DgC virus possesses numerous possible locations for the AAVs to conjugate. We confirmed that the pIX-DgC protein was incorporated into the Ad5-DgC capsid via SDS-PAGE and silver stain **(Fig. 1C)**. In this gel, we also included Ad5-DgC incubated with a 20-fold excess (relative to pIX-DgC copies) of purified DgT-AviTag-MBP protein to verify that the pIX-DgC could react with DgT. By constructing separate pAAV-DJ-VP2-DgT and pAAV-DJ-VP13 plasmids, we inserted DgT into the VP2 protein of AAV-DJ, a structural protein with an average

copy number of 5 per capsid. To make sure that only some of the VP3 proteins (average copy number of 50 per capsid) and VP1 proteins (average copy number of 5 per capsid) would bear DgT, we mutated the VP3's and VP1's ATG start codons in the pAAV-DJ-VP2-DgT plasmid to the weak start codon CTG. Although AAVs can utilize CTG,[22] it leads to less expression compared to ATG. In this way, we constructed an AAV-DJ-DgT vector with VP2-DgT as well as a moderated amount of VP3-DgT, providing a balance between having more available DgT sites and minimizing the negative impact of capsid modifications on production and infectivity. Only a small amount of VP1 was present in the AAV-DJ-DgT capsids (see very faint band), but this did not turn out to preclude infectivity as will be seen later. We could not see VP1-DgT bands, indicating that very little of this protein was produced. We confirmed that AAV-DJ-DgT incorporated VP2-DgT and VP3-DgT using SDS-PAGE with silver staining **(Fig 1D)**. In this gel, we also included AAV-DJ-DgT incubated with a 20-fold excess (relative to VP2-DgT copies) of purified DgC to verify that the VP2-DgT and VP3-DgT could react with DgC. It should be noted that even with the excess of DgC, some unreacted VP2-DgT and VP3-DgT remained, perhaps due to steric shielding effects from the AAV-DJ capsid. To facilitate cell transduction experiments, we constructed our Ad5-DgC to encode eGFP and we provided our AAV-DJ-DgT with a self-complementary genome (to accelerate gene expression) encoding mCherry. We thereby produced and validated the constituent parts of our AdAAV complexes: Ad5-DgC(eGFP) and AAV-DJ-DgT(mCherry).

We next mixed the Ad5-DgC and AAV-DJ-DgT viruses at a 1:10 copy number ratio and incubated overnight at 4°C to induce formation of covalent isopeptide bonds between the viral capsids. Resulting AdAAV complexes were validated using negative stain transmission electron microscopy (TEM) **(Figure 2A)**. We also took TEM images of control mixtures of Ad5 (with unmodified pIX instead of pIX-DgC) and AAV-DJ-DgT **(Figure 2B)** as well as of Ad5-DgC **(Figure S1A)** alone and AAV-DJ-DgT alone **(Figure S1B)**. AdAAV complexes typically featured around 5-15 discernable attached AAVs per adenovirus across multiple separate experiments. Aggregates of more than one AdAAV could be found occasionally as well **(Figure S2)**, though these were uncommon. In the Ad5 + AAV-DJ-DgT mixtures, the viruses usually did not contact each other, though occasionally a single AAV-DJ-DgT capsid could be seen adjacent to an Ad5 **(Figure 2B)**. We surmise that this may have occurred due to weak electrostatic association. These data demonstrate that AdAAV complexes can successfully be made by simply mixing the Ad5-DgC and AAV-DJ-DgT viruses.

We tested the capacity of AdAAV for co-delivering two transgenes into the same cell by leveraging AdAAVs made from Ad5-DgC(eGFP) and AAV-DJ-DgT(mCherry). As mentioned, we provided AAV-DJ-DgT(mCherry) with a self-complementary genome to accelerate gene expression. We infected A549 cells with AdAAV(eGFP, mCherry) complexes, with mixtures of Ad5(eGFP) (bearing unmodified pIX instead of pIX-DgC) and AAV-DJ-DgT(mCherry), with Ad5-DgC(eGFP) alone, and with AAV-DJ-DgT(mCherry) alone. In the AdAAV and Ad5 + AAV-DJ-DgT mixture groups, we used an MOI of 2500 for the Ad component and an MOI of 25000 for the AAV component. In the Ad5 alone group, we used an MOI of 2500. In the AAV-DJ-DgT alone group, we used an MOI of 25000. After 3 days, we imaged the cells via fluorescence microscopy **(Figure S3A)** and utilized flow cytometry to quantify percentages of cells positive for both eGFP and mCherry, for eGFP only, for mCherry only, and for neither. The AdAAV group showed successful co-transduction (eGFP+ and mCherry+) across about 48.7% of the cells **(Figure 2C)**. By comparison, the Ad5 + AAV-DJ-DgT group showed co-transduction in about 33.3% of the cells. It is important to realize that the Ad5 virus displayed higher transduction

efficiency than the Ad5-DgC virus, so the Ad5 + AAV-DJ-DgT control group's co-transduction was artificially inflated. But even though this control group possessed inflated co-transduction, we still observed significantly higher co-transduction with AdAAVs. As a test of whether AdAAVs could enhance co-transduction at a lower MOI, we performed the same experiment using fluorescence microscopy **(Figure S3B)** and flow cytometry, but with MOIs of 500 for the Ad components and 5000 for the AAV components. In this case, we saw an even more pronounced difference between the AdAAV group and the Ad5 + AAV-DJ-DgT control. AdAAVs co-transduced about 9.4% of the cells, while Ad5 + AAV-DJ-DgT co-transduced about 4.1% of the cells **(Figure 2D)**. To gain further perspective on the amount of co-transduction, we compared the percentages of Ad-transduced cells which were also transduced by AAV in the AdAAV and Ad + AAV groups at both MOIs **(Figure 2E)**. At the 2500/25000 MOI level for AdAAV, 72.9% of cells transduced by Ad were also transduced by AAV. At the 2500/25000 MOI level for Ad + AAV, 34.1% of cells transduced by Ad were also transduced by AAV. At the 500/5000 MOI level for AdAAV, 20.8% of cells transduced by Ad were also transduced by AAV. At the 500/5000 MOI level for Ad + AAV, 5.3% of cells transduced by Ad were also transduced by AAV. These differences support the idea that AdAAV has a major advantage in co-transduction capacity compared to Ad + AAV. Our results demonstrate that AdAAV complexes significantly enhance co-transduction and thus could indeed act as a powerful new delivery system for large split transgenes and/or multiple transgenes.

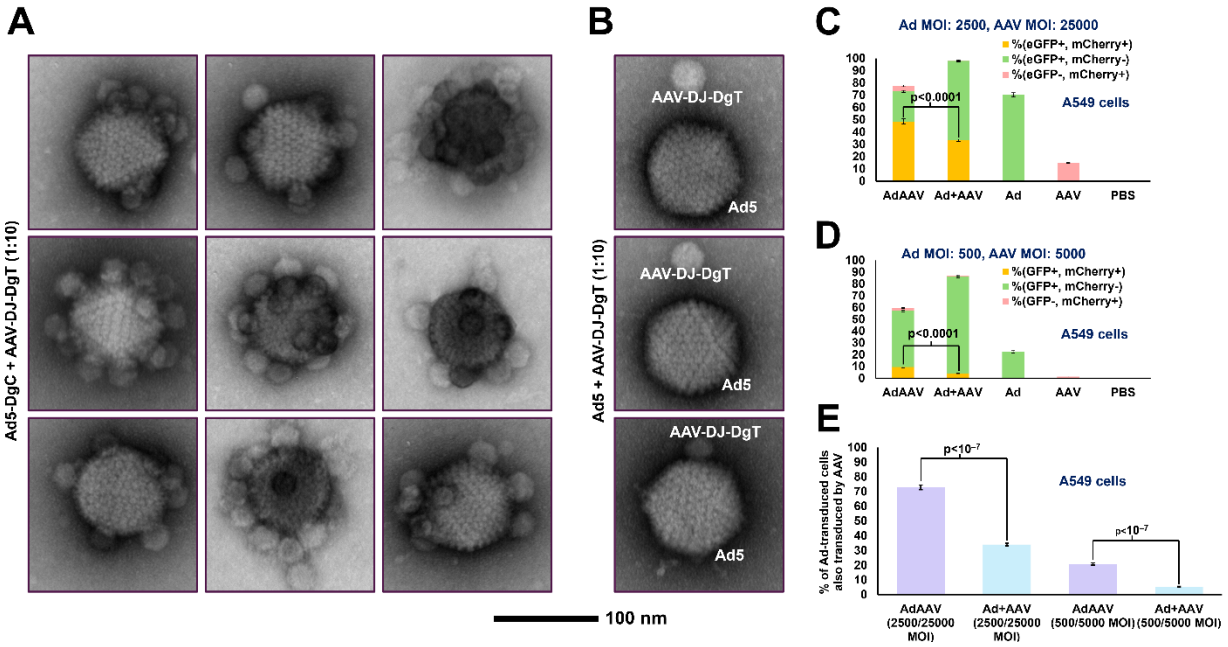

Figure 2 (A) AdAAV complexes formed by mixing Ad5-DgC and AAV-DJ-DgT at a 1:10 ratio and incubating overnight at 4°C, visualized using TEM. AdAAVs typically consist of a single Ad5-DgC and 5-15 covalently bound AAV-DJ-DgT. Nine representative AdAAV complexes are shown. **(B)** Ad5 + AAV-DJ-DgT mixtures subject to the same conditions do not form such complexes. Three representative images of mixtures of Ad5 and AAV-DJ-DgT are shown. **(C)** Flow cytometry quantification of percentages of A549 cells positive for eGFP and mCherry, for eGFP only, for mCherry only, and for neither. Ad component MOI is 2500 and AAV component MOI is 25000. Statistical significance in percentage co-transduction between AdAAV and Ad + AAV groups was evaluated with a two-tailed unpaired t-test. **(D)** Flow cytometry quantification of percentages of A549 cells positive for eGFP and mCherry, for eGFP only, for mCherry only, and for neither. Ad component MOI is 500 and AAV component MOI is 5000. Statistical significance in percentage co-transduction between

AdAAV and Ad + AAV groups was evaluated with a two-tailed unpaired t-test. **(E)** Comparison of the percentages of Ad-transduced cells which were also transduced by AAV across both described MOI levels. Statistical significance between AdAAV and Ad + AAV groups was evaluated with a two-tailed unpaired t-test.

We next sought to test if the advantages of AdAAV would persist in primary human umbilical cord vein endothelial cells (HUVECs), a more challenging target with high physiological relevance. We furthermore reasoned that linking more AAVs per Ad might enhance the amount of achievable co-transduction, so we produced AdAAVs by mixing Ad5-DgC and AAV-DJ-DgT at a 1:50 copy number ratio and incubating overnight at room temperature. We also produced a mixture of Ad5 + AAV-DJ-DgT at a 1:50 copy number ratio as well as Ad5-DgC only and AAV-DJ-DgT only controls with equivalent concentrations of viruses. To evaluate these mixtures, we used TEM. With the larger input of AAVs per Ad, the resultant AdAAVs showed greatly increased numbers of AAVs (~10-30) linked to each Ad capsid **(Figure 3A)**. As expected, control Ad5 + AAV-DJ-DgT mixtures only occasionally showed colocalization of Ad and AAV, likely by chance or by weak electrostatic interactions **(Figure 3B)**. These data illustrate the easy customizability of AdAAVs through alteration of Ad to AAV ratio.

We then infected HUVECs with the AdAAV(eGFP, mCherry) complexes, with the mixtures of Ad5(eGFP) and AAV-DJ-DgT(mCherry), with Ad5-DgC(eGFP) alone, and with AAV-DJ-DgT(mCherry) alone. In the AdAAV and Ad5 + AAV-DJ-DgT mixture groups, we chose an MOI of 400 for the Ad component and an MOI of 20000 for the AAV component. In the Ad5 alone group, we used an MOI of 400. In the AAV-DJ-DgT alone group, we used an MOI of 20000. We chose these low MOIs to illustrate the strength of the AdAAV platform for facilitating co-transduction at low doses. After 3 days, we imaged the cells using fluorescence microscopy **(Figure S4)** and employed flow cytometry to quantify percentages of cells positive for both eGFP and mCherry, for eGFP only, for mCherry only, and for neither. The AdAAV group again demonstrated significantly higher co-transduction (eGFP+ and mCherry+) across 1.92% of the cells by comparison to the Ad5 + AAV-DJ-DgT group which only co-transduced 0.98% of the cells. As mentioned earlier, it is important to realize that the Ad5 virus displayed higher transduction efficiency than the Ad5-DgC virus, so the Ad5 + AAV-DJ-DgT control group's co-transduction was somewhat inflated. Despite this, we still observed significantly higher co-transduction with AdAAVs. Once again, to obtain further perspective on the amount of co-transduction, we compared percentages of Ad-transduced cells which were also transduced by AAV in the AdAAV and Ad + AAV groups. We found for AdAAV that 36.1% of HUVECs transduced by Ad were also transduced by AAV whereas for Ad + AAV 16.2% of HUVECs transduced by Ad were also transduced by AAV. These results in primary cells provide further evidence that AdAAV can act as a potent vehicle for delivery of large split genes or for multigenic delivery.

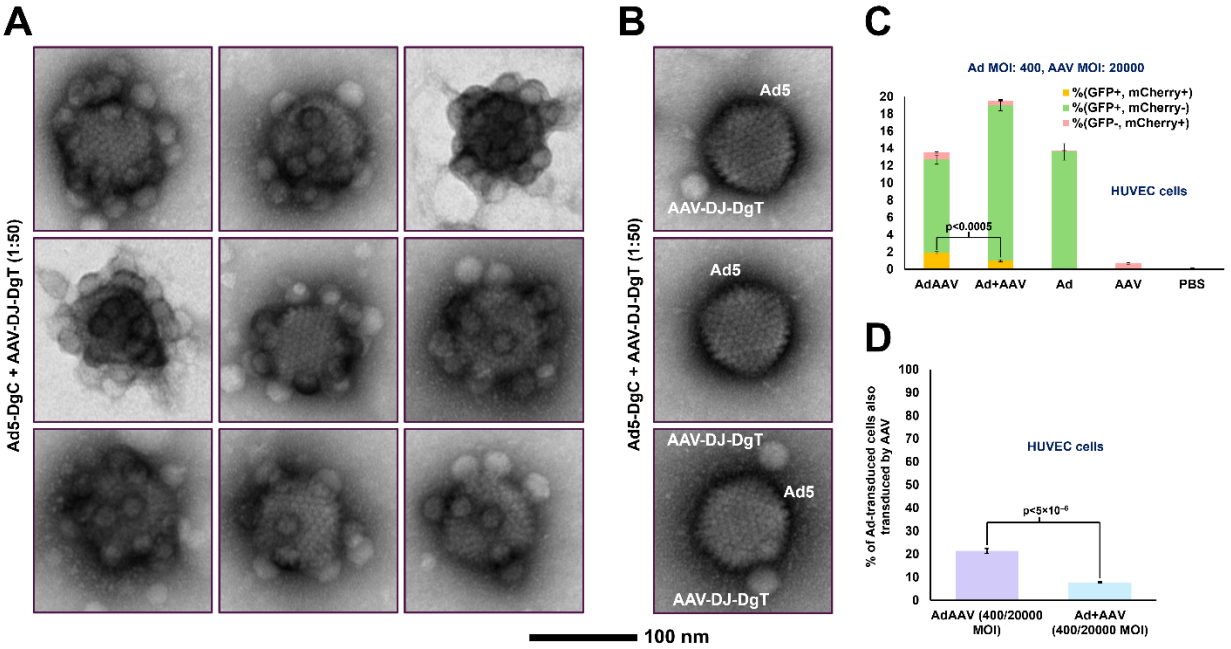

Figure 3 (A) AdAAV complexes formed by mixing Ad5-DgC and AAV-DJ-DgT at a 1:50 ratio and incubating overnight at room temperature, visualized using TEM. These AdAAVs typically consist of a single Ad5-DgC and 10-30 covalently bound AAV-DJ-DgT. Nine representative AdAAV complexes are shown. **(B)** Ad5 + AAV-DJ-DgT mixtures subject to the same conditions do not form complexes. Three representative images of mixtures of Ad5 and AAV-DJ-DgT are shown. **(C)** Flow cytometry quantification of percentages of primary HUVECs positive for eGFP and mCherry, for eGFP only, for mCherry only, and for neither. Ad component MOI is 400 and AAV component MOI is 20000. Statistical significance in percentage co-transduction between AdAAV and Ad + AAV groups was evaluated with a two-tailed unpaired t-test. **(D)** Comparison of the percentages of Ad-transduced cells which were also transduced by AAV at the described MOI level. Statistical significance between AdAAV and Ad + AAV groups was evaluated with a two-tailed unpaired t-test.

Discussion

Our data suggest that AdAAV represents a new platform technology for gene therapy, particularly in the area of enhancing co-delivery of split genetic cargos. We demonstrate incorporation of pIX-DgC into the Ad5 capsid and VP2-DgT and VP3-DgT (but not a measurable amount of VP1-DgT) into the AAV-DJ capsid via SDS-PAGE silver stain. We also utilize SDS-PAGE silver stain to show that the pIX-DgC reacts to form a covalent linkage with purified DgT-AviTag-MBP as well as that VP2-DgT and VP3-DgT react to form covalent linkages with purified DgC. We validate successful formation of AdAAV complexes by TEM. Finally, we demonstrate enhanced co-delivery of two transgenes, eGFP in the Ad component and mCherry in the AAV component. We showed enhanced co-delivery results in both immortalized A549 cells and primary HUVECs, indicating broad physiological relevance for AdAAV constructs. Since we observed 5-15 AAVs per Ad for the 1:10 (Ad to AAV ratio) AdAAVs and 10-30 AAVs per Ad for the 1:50 (Ad to AAV ratio) AdAAVs, the vectors likely could deliver a mixture of several distinct AAV cargos in addition to Ad cargo. AdAAVs might eventually deliver split gene products in a fashion similar to that of dual and triple AAVs, but with the advantage of greatly enhanced co-delivery efficiency.

As a future direction, we envision AdAAVs as a superlative platform for multigenic CRISPR-Cas gene insertion. Because of the double-stranded DNA (dsDNA) genome of Ad, any Ad vector on its own will have difficulty with efficient CRISPR-mediated knock-in of genes via

homology directed repair (HDR).[23] Indeed, dsDNA templates are less efficient and more prone to off-target integration. However, Ad's higher packaging capacity makes it better suited for carrying large Cas protein genes in addition to several guide RNA (gRNA) genes. By contrast, AAV features a single-stranded DNA (ssDNA) genome with a lower packaging capacity. Further iterations of AdAAV may therefore capitalize on the advantages of both vectors, leveraging the Ad to encode a Cas protein and several gRNAs while employing a mixture of AAVs to carry multiple ssDNA donor templates. Alternatively, the Ad component could encode base editors, prime editors, epigenome editors, recombinases, or other machinery that are too large to fit into a single AAV capsid.[24] CRISPR AdAAVs may someday programmably and efficiently insert multiple transgenes into targeted locations within the human genome, facilitating powerful gene editing therapies for complex diseases.

Methods

Production of Ad5-DgC

We made Ad5-DgC by first cloning a fragment containing a linker-pIX-DgC sequence directly into an Ad5 genomic plasmid (E1/E3-deleted Ad5 backbone) via Gibson assembly. The linker was a 45 amino acid rigid spacer derived from the linkers described by Vellinga et al.[25] After verifying sequence correctness of the resulting Ad5-DgC genomic DNA, we linearized the plasmid and transfected it into HEK293 cells. Serial passages of infection with cell lysate supernatant (lysis was achieved by 4 freeze-thaw cycles per passage) were used to upscale the virus into larger and larger cell culture vessels. We eventually infected 20 T175 flasks with the lysate supernatant from a single T175 flask. After observing approximately 50% cell detachment, we pelleted the cells, performed a final set of 4 freeze-thaw cycles, and loaded the supernatant onto CsCl gradients consisting of 4 mL layer of 1.33 g/cm^3 CsCl on top of a 4 mL layer of 1.45 g/cm^3 CsCl. We ultracentrifuged the gradient at 20,000 rpm for 4 hours and then extracted the band corresponding to intact Ad5-DgC particles. This band was loaded onto another CsCl gradient of the same composition and ultracentrifuged at 25,000 rpm for 18 hours. The band was extracted and injected into a Thermo Scientific Slide-A-Lyzer G2 Dialysis Cassette. Dialysis was performed in 1 L of PBS with 10% glycerol buffer for 2 hours before exchanging for fresh buffer to facilitate another 2 hours of dialysis. Finally, the purified Ad5-DgC was withdrawn from the dialysis cassette, aliquoted into 1.5 mL tubes, and stored at –80°C until use. Titration of Ad5-DgC was accomplished using UV-visible spectroscopy.

Production of AAV-DJ-DgT

To make AAV-DJ-DgT, we first constructed pAAV-DJ-VP13 and pAAV-DJ-VP2-DgT plasmids through cloning with Gibson assembly. As part of our cloning strategy and to ensure that only a moderate fraction of the VP3 and VP1 proteins would be expressed as VP3-DgT and VP1-DgT, we mutated the VP3 and VP1 start codons from ATG to CTG in the pAAV-DJ-VP2-DgT plasmid. For the pAAV-DJ-VP13 plasmid, we used a mutation in the VP2 start codon from ACG to GCG to ensure that expression of only VP1 and VP3 would occur. For the pAAV-DJ-VP2-DgT plasmid, we added a sequence encoding a pair of short flexible linkers flanking the DgT peptide after position 453 in the *Cap* sequence. We employed a self-complementary transfer plasmid encoding mCherry driven by a CAG promoter, pscAAV(mCherry). Next, AAV-DJ-DgT was produced with the help of the viral vector core at UMass Chan Medical School. The core facility transfected HEK293T cells with 0.3 mg of pAAV-DJ-VP13, 1.5 mg of pAAV-DJ-VP2-

DgT, 0.75 mg of pscAAV(mCherry), and 0.75 mg of a pAdΔF6 helper plasmid before purification by iodixanol gradient ultracentrifugation. Titration of the self-complementary AAV-DJ-DgT was accomplished using digital droplet PCR.

SDS-PAGE silver stain, AdAAV assembly, and TEM validation

SDS-PAGE was carried out by running samples on Criterion™ precast gels from Bio-Rad at 50 mA for 1 hour. After removing the gels from their holders, we performed silver stains using a Pierce™ silver stain kit. The first batch of AdAAVs was assembled by mixing Ad5-DgC(eGFP) with self-complementary AAV-DJ-DgT(mCherry) at a 1:10 ratio and incubating overnight at 4°C. Ad5(eGFP) + self-complementary AAV-DJ-DgT(mCherry) controls as well as Ad5-DgC(eGFP) only controls and self-complementary AAV-DJ-DgT(mCherry) only controls were mixed and incubated in the same way. The second batch of AdAAVs was assembled by mixing Ad5-DgC(eGFP) with self-complementary AAV-DJ-DgT(mCherry) at a 1:50 ratio and incubating overnight at room temperature. Ad5(eGFP) + self-complementary AAV-DJ-DgT(mCherry) controls as well as Ad5-DgC(eGFP) only controls and self-complementary AAV-DJ-DgT(mCherry) only controls were mixed and incubated in the same way. For transmission electron microscopy (TEM) validation, a small volume of each group (Ad5-DgC + AAV-DJ-DgT, Ad5 + AAV-DJ-DgT, Ad5-DgC only, AAV-DJ-DgT only) was transferred to a separate tube, diluted 1:10 in PBS with 10% glycerol, negatively stained using 1% uranyl acetate, and imaged by TEM.

Co-transduction assays

To measure the efficacy of co-transduction in A549 cells, 1×10^4 cells per well were seeded in a 96-well plate 4 hours before infection. AdAAV, Ad5 + AAV-DJ-DgT (Ad +AAV), Ad5-DgC only, and AAV-DJ-DgT only (all from the 1:10 Ad to AAV ratio batch) were each added to five replicate wells containing cells at the MOI values specified in the Results section. 3 days after infection, we imaged the cells by fluorescence microscopy. Next, the cells were detached using trypsinization and flow cytometry was utilized to quantify the percentages in each well of cells positive for both eGFP and mCherry, of cells positive for only eGFP, of cells positive for only mCherry, and of cells positive for neither. Statistical significance of co-transduction comparisons between AdAAV and Ad5 + AAV-DJ-DgT (Ad + AAV) groups was evaluated using a two-tailed unpaired t-test.

To measure the efficacy of co-transduction in HUVECs, 2×10^4 cells per well were seeded in a 96-well plate 4 hours before infection. AdAAV, Ad5 + AAV-DJ-DgT (Ad +AAV), Ad5-DgC only, and AAV-DJ-DgT only (all from the 1:50 Ad to AAV ratio batch) were each added to five replicate wells containing cells at the MOI values specified in the Results section. 3 days after infection, we imaged the cells by fluorescence microscopy. Next, the cells were detached using trypsinization and flow cytometry was utilized to quantify the percentages in each well of cells positive for both eGFP and mCherry, of cells positive for only eGFP, of cells positive for only mCherry, and of cells positive for neither. Statistical significance of co-transduction comparisons between AdAAV and Ad5 + AAV-DJ-DgT (Ad + AAV) groups was evaluated using a two-tailed unpaired t-test.

Acknowledgements

We thank the viral vector core at UMass Chan Medical School for their assistance in producing AAV-DJ-DgT vectors.

References

1. Collins, L. T., Ponnazhagan, S. & Curiel, D. T. Synthetic Biology Design as a Paradigm Shift toward Manufacturing Affordable Adeno-Associated Virus Gene Therapies. *ACS Synth. Biol.* **12**, 17–26 (2023).
2. Philippidis, A. BioMarin's ROCTAVIAN Wins Food and Drug Administration Approval As First Gene Therapy for Severe Hemophilia A. *Hum. Gene Ther.* **34**, 665–668 (2023).
3. Kasimsetty, A. & Sabatino, D. E. Integration and the risk of liver cancer—Is there a real risk? *J. Viral Hepat.* **31**, 26–34 (2024).
4. Wang, J.-H., Gessler, D. J., Zhan, W., Gallagher, T. L. & Gao, G. Adeno-associated virus as a delivery vector for gene therapy of human diseases. *Signal Transduct. Target. Ther.* **9**, 78 (2024).
5. Zhi, S. *et al.* Dual-AAV delivering split prime editor system for in vivo genome editing. *Mol. Ther.* **30**, 283–294 (2022).
6. Trapani, I., Tornabene, P. & Auricchio, A. Large gene delivery to the retina with AAV vectors: are we there yet? *Gene Ther.* **28**, 220–222 (2021).
7. Ghosh, A. & Duan, D. Expanding adeno-associated viral vector capacity: a tale of two vectors. *Biotechnol. Genet. Eng. Rev.* **24**, 165–178 (2007).
8. Tornabene, P. & Trapani, I. Can Adeno-Associated Viral Vectors Deliver Effectively Large Genes? *Hum. Gene Ther.* **31**, 47–56 (2020).
9. Akil, O. Dual and triple AAV delivery of large therapeutic gene sequences into the inner ear. *Hear. Res.* **394**, 107912 (2020).
10. Maddalena, A. *et al.* Triple Vectors Expand AAV Transfer Capacity in the Retina. *Mol. Ther.* **26**, 524–541 (2018).
11. Patel, A., Zhao, J., Duan, D. & Lai, Y. Design of AAV Vectors for Delivery of Large or Multiple Transgenes BT - Adeno-Associated Virus Vectors: Design and Delivery. in (ed. Castle, M. J.) 19–33 (Springer New York, 2019). doi:10.1007/978-1-4939-9139-6_2.
12. Meier, A. F., Fraefel, C. & Seyffert, M. The Interplay between Adeno-Associated Virus and Its Helper Viruses. *Viruses* vol. 12 at https://doi.org/10.3390/v12060662 (2020).
13. Keeble, A. H. *et al.* DogCatcher allows loop-friendly protein-protein ligation. *Cell Chem. Biol.* **29**, 339-350.e10 (2022).
14. Collins, L. T. & Curiel, D. T. Synthetic Biology Approaches for Engineering Next-Generation Adenoviral Gene Therapies. *ACS Nano* (2021) doi:10.1021/acsnano.1c04556.
15. Vaiserman, A., De Falco, E., Koliada, A., Maslova, O. & Balistreri, C. R. Anti-ageing gene therapy: Not so far away? *Ageing Res. Rev.* **56**, 100977 (2019).
16. Khatib, T. Z. *et al.* Receptor-ligand supplementation via a self-cleaving 2A peptide–based gene therapy promotes CNS axonal transport with functional recovery. *Sci. Adv.* **7**, eabd2590 (2021).
17. Kitada, T., DiAndreth, B., Teague, B. & Weiss, R. Programming gene and engineered-cell therapies with synthetic biology. *Science (80-.).* **359**, eaad1067 (2018).
18. Higashikuni, Y., Chen, W. C. W. & Lu, T. K. Advancing therapeutic applications of synthetic gene circuits. *Curr. Opin. Biotechnol.* **47**, 133–141 (2017).
19. Kemmer, C. *et al.* Self-sufficient control of urate homeostasis in mice by a synthetic circuit. *Nat. Biotechnol.* **28**, 355–360 (2010).
20. Wörner, T. P. *et al.* Adeno-associated virus capsid assembly is divergent and stochastic. *Nat. Commun.* **12**, 1642 (2021).

21. Meulenbroek, R. A., Sargent, K. L., Lunde, J., Jasmin, B. J. & Parks, R. J. Use of adenovirus protein IX (pIX) to display large polypeptides on the virion - generation of fluorescent virus through the incorporation of pIX-GFP. *Mol. Ther.* **9**, 617–624 (2004).
22. Chen, H. Adeno-associated virus vectors for human gene therapy. *World J. Med. Genet.* **5**, 28–45 (2015).
23. Iyer, S. *et al.* Efficient Homology-Directed Repair with Circular Single-Stranded DNA Donors. *Cris. J.* **5**, 685–701 (2022).
24. Madigan, V., Zhang, F. & Dahlman, J. E. Drug delivery systems for CRISPR-based genome editors. *Nat. Rev. Drug Discov.* **22**, 875–894 (2023).
25. Vellinga, J. *et al.* Spacers Increase the Accessibility of Peptide Ligands Linked to the Carboxyl Terminus of Adenovirus Minor Capsid Protein IX. *J. Virol.* **78**, 3470 LP – 3479 (2004).

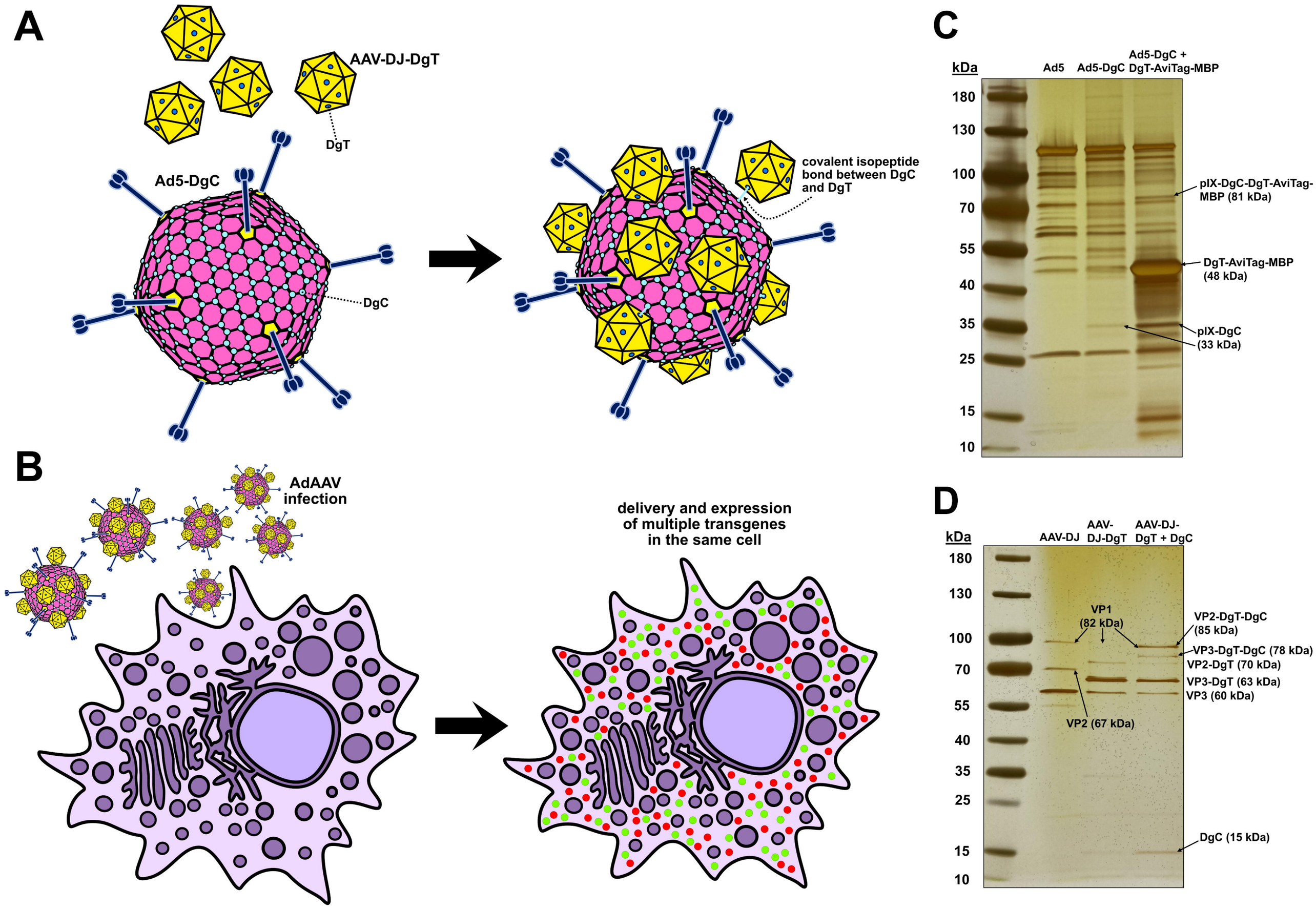
A
AAV-DJ-DgT
DgT
Ad5-DgC
DgC
covalent isopeptide bond between DgC and DgT
B
AdAAV infection
delivery and expression of multiple transgenes in the same cell
C
kDa
Ad5
Ad5-DgC
Ad5-DgC + DgT-AviTag-MBP
180
130
100
70
55
40
35
25
15
10
pIX-DgC-DgT-AviTag-MBP (81 kDa)
DgT-AviTag-MBP (48 kDa)
pIX-DgC (33 kDa)
D
kDa
AAV-DJ
AAV-DJ-DgT
AAV-DJ-DgT + DgC
180
130
100
70
55
40
35
25
15
10
VP1 (82 kDa)
VP2-DgT-DgC (85 kDa)
VP3-DgT-DgC (78 kDa)
VP2-DgT (70 kDa)
VP3-DgT (63 kDa)
VP3 (60 kDa)
VP2 (67 kDa)
DgC (15 kDa)

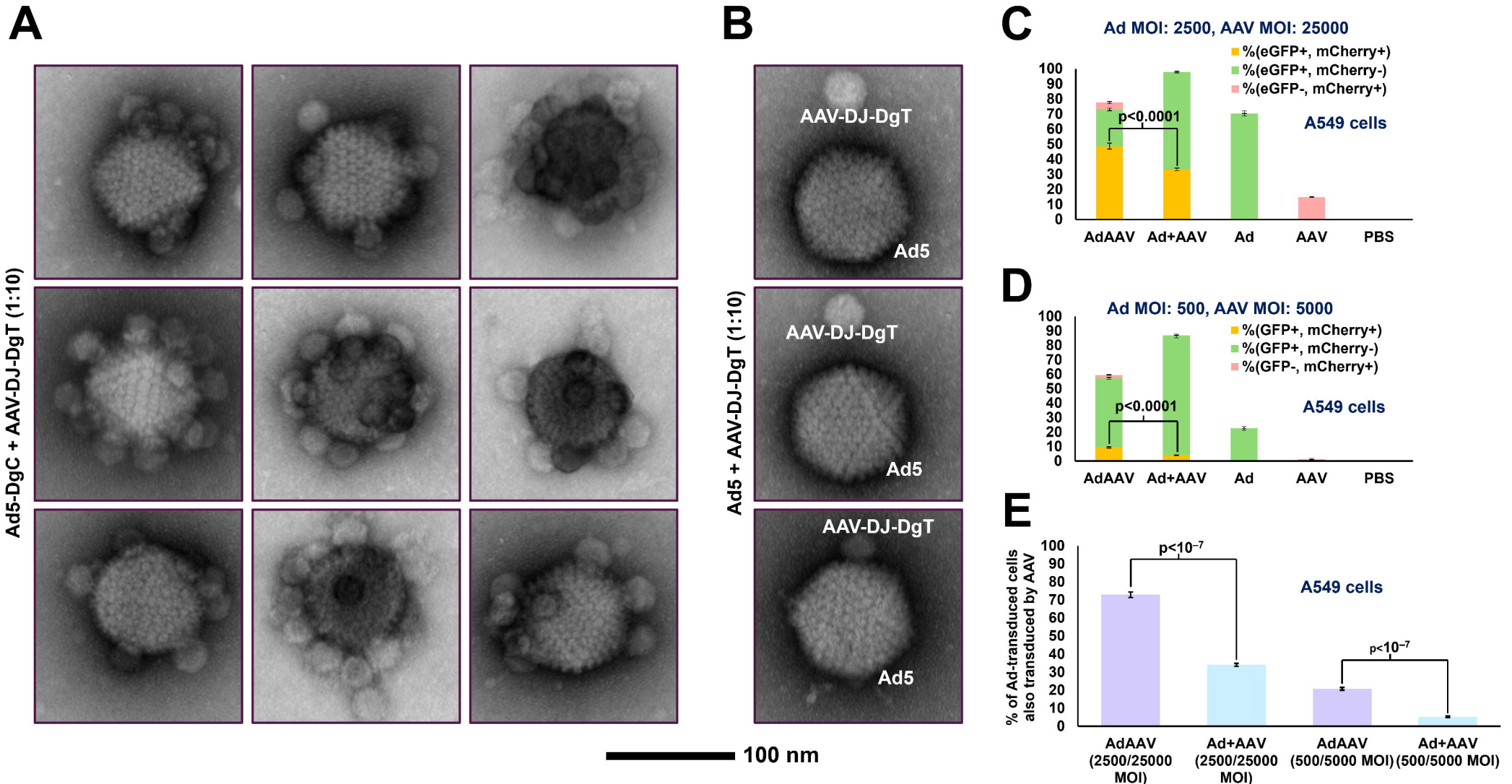
A
Ad5-DgC + AAV-DJ-DgT (1:10)
B
Ad5 + AAV-DJ-DgT (1:10)
AAV-DJ-DgT
Ad5
AAV-DJ-DgT
Ad5
AAV-DJ-DgT
Ad5
100 nm
C
Ad MOI: 2500, AAV MOI: 25000
%(eGFP+, mCherry+)
%(eGFP+, mCherry-)
%(eGFP-, mCherry+)
p<0.0001
A549 cells
AdAAV
Ad+AAV
Ad
AAV
PBS
D
Ad MOI: 500, AAV MOI: 5000
%(GFP+, mCherry+)
%(GFP+, mCherry-)
%(GFP-, mCherry+)
p<0.0001
A549 cells
AdAAV
Ad+AAV
Ad
AAV
PBS
E
% of Ad-transduced cells also transduced by AAV
p<10⁻⁷
p<10⁻⁷
A549 cells
AdAAV (2500/25000 MOI)
Ad+AAV (2500/25000 MOI)
AdAAV (500/5000 MOI)
Ad+AAV (500/5000 MOI)

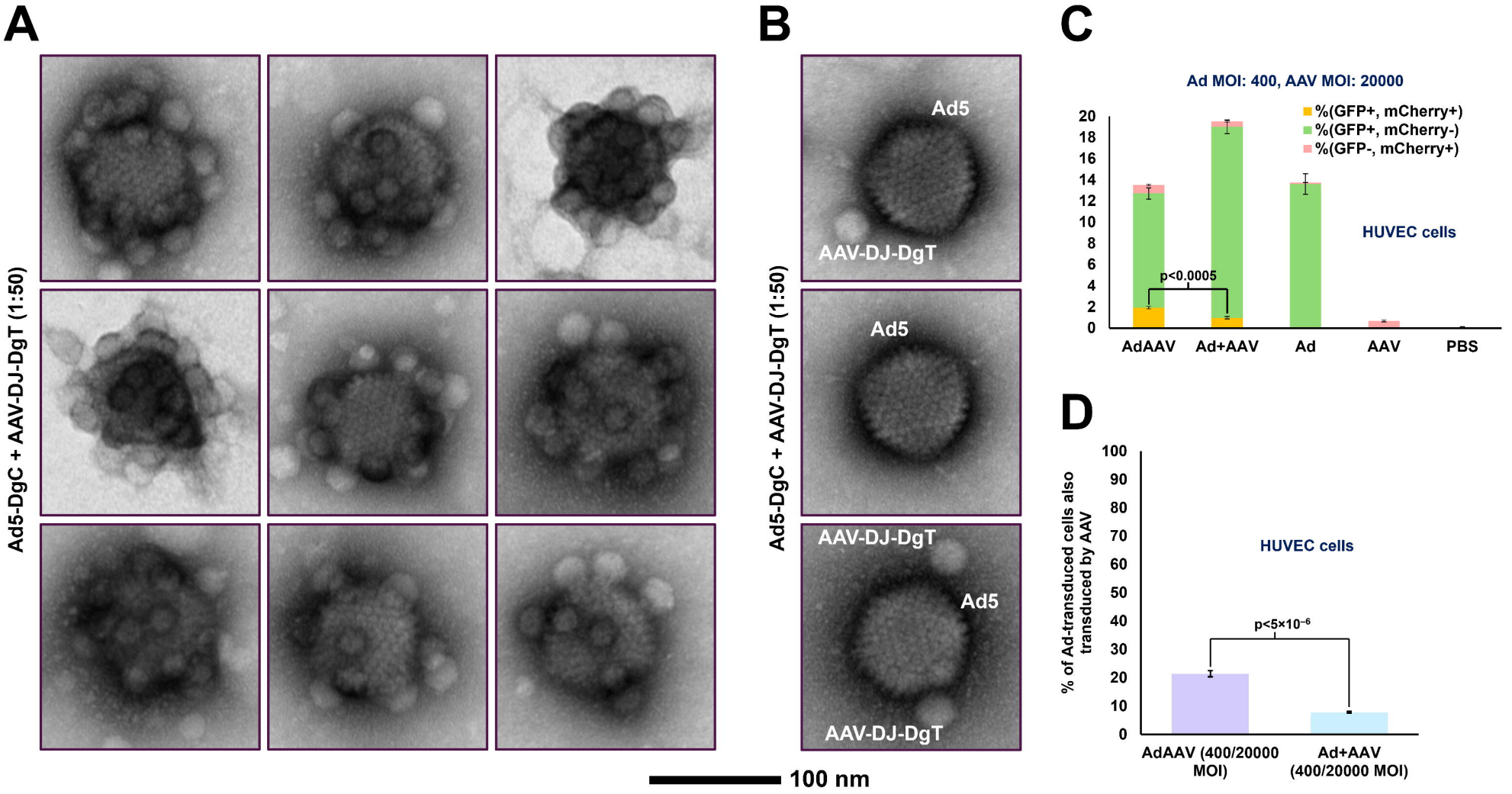
A
Ad5-DgC + AAV-DJ-DgT (1:50)
B
Ad5-DgC + AAV-DJ-DgT (1:50)
Ad5
AAV-DJ-DgT
Ad5
AAV-DJ-DgT
Ad5
AAV-DJ-DgT
100 nm
C
Ad MOI: 400, AAV MOI: 20000
%(GFP+, mCherry+)
%(GFP+, mCherry-)
%(GFP-, mCherry+)
HUVEC cells
p<0.0005
AdAAV
Ad+AAV
Ad
AAV
PBS
D
% of Ad-transduced cells also transduced by AAV
HUVEC cells
p<5×10⁻⁶
AdAAV (400/20000 MOI)
Ad+AAV (400/20000 MOI)